Available online at www.sciencedirect.com
ScienceDirect
Chemical Physics Letters 445 (2007) 117–124
CHEMICAL PHYSICS LETTERS
www.elsevier.com/locate/cplett

A density functional theory study of the hydrogen bond interactions in glycine dimers

Mariana F. de Carvalho [a], Ricardo A. Mosquera [b], Roberto Rivelino [a,*]

[a] *Instituto de Física, Universidade Federal da Bahia, 40210-340 Salvador, Bahia, Brazil*
[b] *Departamento de Química Física, Facultade de Química, Universidade de Vigo, 36310 Vigo, Galicia, Spain*

Received 8 May 2007; in final form 27 July 2007
Available online 6 August 2007

Abstract

We report a theoretical study on the stability and bonding of glycine dimers using diverse DFT functionals (B3LYP, B3PW91, mPW1PW91, and MPW1B95) and MP2 calculations. It comprises the determination of the optimized structures, relative stabilities, corrected binding energies, and vibrational spectra of four different dimers, whose electron densities are analyzed using the Quantum Theory of Atoms in Molecules. DFT functionals show the cyclic planar dimer with two O–H···O hydrogen bonds as the most stable and the most strongly bound structure. They find the stacked dimer between 1.7 and 4.7 kcal/mol higher, whereas it is the most stable with MP2.

1. Introduction

The conformational stability of the three-dimensional structure of protein sequences has long been recognized to play an important role for the biological properties of polypeptide chains [1]. Conformational equilibrium is known to be responsible for folding, properties, and functions of peptides and proteins [2–7]. Essentially, this dynamical process is in connection with the molecular behavior of their basic constituents: the amino acids. Thus, the description of intra and intermolecular interactions involving the amino acid residues is among the main challenges to investigate the biochemistry of proteins. Usually, the simplest amino acid structural unit (NH_2–CH_2–COOH, glycine molecule) has been employed as a prototype to understand the conformational arrangements in larger systems [3,4] and the interactions between amino acids and water [8–10].

A great variety of conformations of isolated glycine has been identified via microwave spectroscopy and investigated by combining ab initio calculations [11–13]. Also, electron momentum spectroscopy has been employed to access the electron density distribution in glycine conformers [14]. The diversity of proton acceptors and donors, and the number of different spatial arrangements with rather low relative molecular energy in glycine, results in a large number of possible dimers. For example, those stabilized by interactions linking amino hydrogen atoms to the carbonyl oxygen lone pairs, the hydroxyl hydrogen to the amino nitrogen lone pair, or amino hydrogen atoms to the hydroxyl oxygen lone pairs in several fashions. Thus, the existence of various aggregates stabilized by hydrogen bonds is expected for glycine. In this sense, dimers of glycine have been a recent issue of theoretical and experimental studies [15]. There is, however, a lack of research on glycine dimers in terms of the properties of their hydrogen bonds [16,17].

This Letter investigates the intermolecular interactions involved in glycine dimerization. Thus, we have studied the interaction energies and electron density variations in four possible dimers, which show different patterns of hydrogen bonding [15]. The electronic structure calculations were carried out using diverse approaches of the density functional theory (DFT) [18], which have been proven to provide accurate structural and energetic description

* Corresponding author. Fax: +55 71 3283 6606.
E-mail address: rivelino@ufba.br (R. Rivelino).

0009-2614/$ - see front matter © 2007 Elsevier B.V. All rights reserved.
doi:10.1016/j.cplett.2007.07.077

for both neutral and ionic amino acids in gas phase [19], as well as for other hydrogen-bonded systems [20,21]. We have also carried out a topological electron density study on the hydrogen bond formation within the framework of the Quantum Theory of Atoms in Molecules (QTAIM) [22].

2. Methods and calculations

The calculations were carried out using current density functional methods [18] as implemented in the GAUSSIAN 98 [23] and 03 [24] packages. The geometries of four glycine dimers (named I–IV in Fig. 1) were fully optimized in the supermolecular approach as follows: using Becke's three parameter functional [25] with (i) the Lee–Yang–Parr correlation (B3LYP) [26] and (ii) Perdew–Wang's 91 correlation functionals (B3PW91) [27]; and using Barone–Adamo's one parameter with the modified Perdew–Wang's 91 exchange and correlation functionals (mPW1PW91) [27–29]. We have also employed the meta hybrid DFT method MPW1B95, recently developed by Zhao and Truhlar [30], which has shown to provide reliable descriptions of complexes due to weak interactions, like hydrogen bonding aggregates [30]

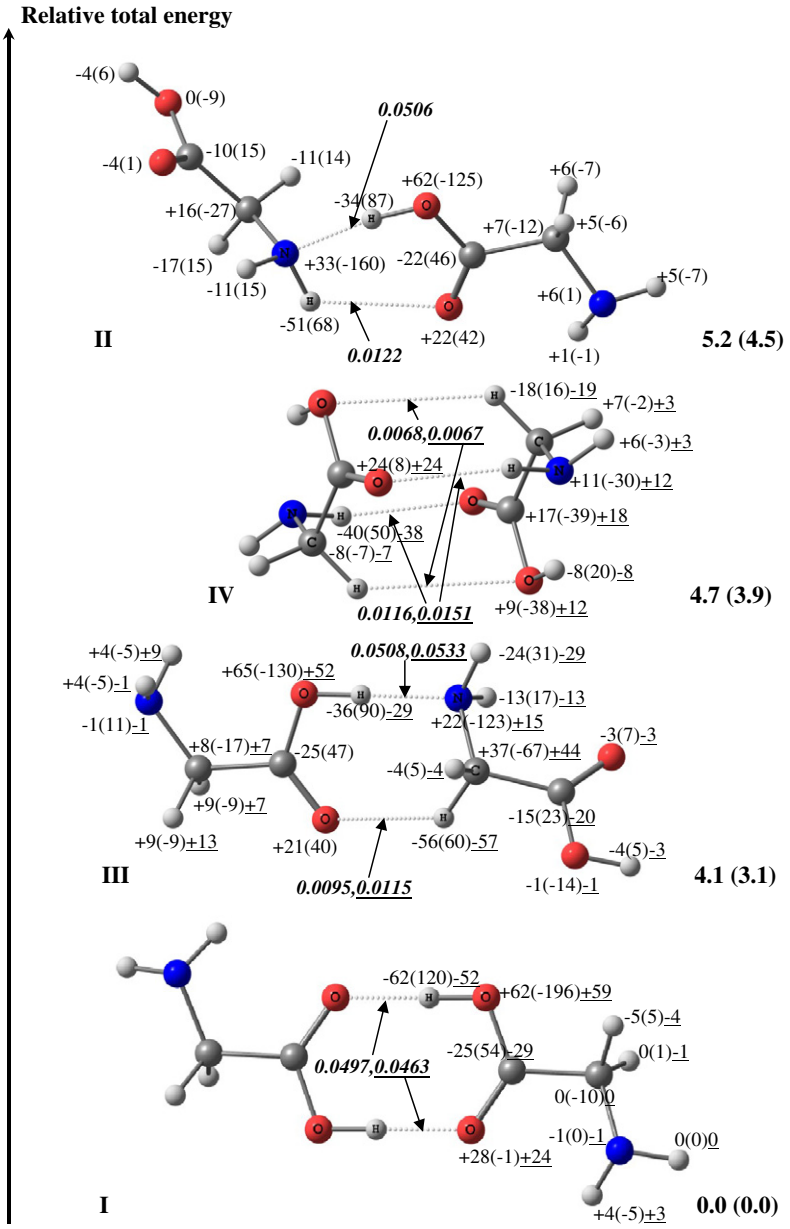

Fig. 1. Optimized structures for different glycine dimers (I–IV). The calculated relative stabilities according to B3LYP/aug-cc-pVDZ total energy are given (in kcal mol^{-1}) in boldface at the right (values in parentheses correspond to the B3LYP/6-311+G(d,p) level). $\Delta N(\Omega)$ (in a.u. multiplied by 10^3) and $\Delta E(\Omega)$ values (in kJ mol^{-1} and written in parenthesis) computed from MPW1B95/aug-cc-pVTZ electron densities are shown for every atom. Values of the electron density at the bond critical points associated to hydrogen bonds are written in italics (in au). Quantities obtained with MP2/aug-cc-pVDZ electron densities are underlined. $\Delta E(\Omega)$ values obtained with AIMPAC from the MP2 electron densities are not used in our discussion as their summation cannot recover the corresponding electronic molecular energies.

and π–π stacking complexes [31], features that should be essential for studying glycine dimers. To compare the DFT results, we additionally perform the second-order Møller–Plesset perturbation theory (MP2) with the frozen core approximation.

Two basis sets were employed with the usual functionals: the triple-zeta split-valence 6-311+G(d,p), and the augmented correlation-consistent polarized double-zeta split-valence, aug-cc-pVDZ. At the MP2 level, only the latter basis set was employed. The MPW1B95 method was only used in connection with the aug-cc-pVTZ basis set, as the developers of this method pointed out that it should be useable without the need of counterpoise corrections, especially when the basis is triple-zeta quality or better [30]. We have considered the correction for basis set superposition error (BSSE), using the counterpoise technique [32,33], and the nuclear relaxation energy (NRE) of the monomers upon complexation, for computing the interaction energy of the glycine dimers. This was determined as the energy differences between the optimized monomers and the ones having the same geometry in the dimer structure. Also, the vibrational frequencies were determined analytically in the harmonic approximation, so that the complexation energies were also calculated considering the differences in zero-point vibrational energy (ΔZPVE).

The QTAIM analysis was carried out using the AIMPAC program [34] on MPW1B95/aug-cc-pVTZ and MP2/aug-cc-pVTZ electron densities for all the dimers and the conformers of the monomer of glycine that can be distinguished in them. The conformers of glycine monomer are named by an acronym made from the approximated values (*A* for anti, *S* for syn, and *G* for values around to ±90°) of its main dihedral angles ($\omega_1 = $ H–O–C–C, $\omega_2 = $ O–C–C–N, $\omega_3 = $ C–C–N–*lp*). Therefore, we could say that dimers I and II are made up of two *AAG* monomers, dimer III comes from the interaction between *ASA* and *AAA* monomers, and dimer IV contains two *SSS* monomers. In all cases, the summations of atomic electron populations, $N(\Omega)$, recover the total molecular electron population within 5×10^{-4} au. The summations of atomic energies, $E(\Omega)$, obtained from DFT electron densities recover the electronic molecular energies within 0.9 kJ mol^{-1}. $E(\Omega)$ values obtained from MP2 electron densities are not used in this work as it is known they do not recover the corresponding molecular energy. Fig. 1 shows the relative atomic electron populations, $\Delta N(\Omega)$, and energies, $\Delta E(\Omega)$, with regard to those in the corresponding monomer. Values of the electron density at the H-bond critical points, ρ_{HB}, are also shown and commented below in relation to the H-bond strength.

3. Results and discussion

3.1. Structural and energetic aspects

The geometries of the glycine dimers I–IV were firstly obtained with three usual DFT functionals; i.e. B3LYP, B3PW91, and mPW1PW91 combined with the 6-311+G(d,p) and aug-cc-pVDZ basis sets. Also the calculations were carried out at the MPW1B95/aug-cc-pVTZ and MP2/auc-cc-pVDZ levels. Table 1 summarizes all calculated hydrogen bond distances, rotational constants, and dipole moments of the different dimers. The optimized structures are presented in Fig. 1, considering their relative stabilities with respect to the lowest calculated total energy (at the B3LYP/aug-cc-pVDZ level). As shown in Table 2, the most stable structure obtained with DFT was found for dimer I that exhibits a cyclic planar geometry with two linear O–H···O=C intermolecular hydrogen bonds acting cooperatively. These distances were calculated in the range of 1.6–1.7 Å (see Table 1), using all methods described here. Conversely, at the MP2 level dimer IV was found to be 1.33 kcal/mol more stable than dimer I. Also, dimer II was not found as a stable glycine dimer using this level of theory.

Considering the DFT results described in this study, the smallest difference of relative stability from dimer I to the second lowest energy structure (dimer IV) in our series was ca. 1.7 kcal/mol at the MPW1B95/aug-cc-pVTZ level. Nevertheless, it has to be stressed that the relative sequence of stabilities is altered by the remaining computational levels. All of DFT methods show dimer III as the second most stable if we exclude mPW1PW91/aug-cc-pVDZ calculations, which provide very similar energies for dimers II and III. Also, if we exclude MPW1B95, the difference between the total electronic energy of dimers III and IV is below 1 kcal mol^{-1} and it is reduced when extending the basis set.

On the other hand, for dimer II all DFT levels of calculation considered here yielded the highest-energy structure with relative stability going from ca. 4.4 to 5.2 kcal mol^{-1}, compared to dimer I. Effectively, the hydrogen bonding pattern in dimer II (Fig. 1) seems to be much less favored in comparison with the other glycine dimer structures. Indeed, this structure is not favored in the MP2/aug-cc-pVDZ calculation. Comparing II and III, the O–H···N< hydrogen bonds are calculated around 1.7 Å in both cases, considering the DFT levels of calculation given in Table 1. Also, the N–H···O=C (dimer II) and C–H···O=C (dimer III) hydrogen bonds give very similar values of 2.4 Å. In the case of dimer IV, a stacked structure is formed with antiparallel dipole–dipole interaction giving a residual dipole moment, calculated as only 0.002 D at the mPW1PW91/aug-cc-pVDZ level, and bound by two N–H···O=C hydrogen bonds (calculated as ca. 2.3 Å) and two weak C–H···O–H hydrogen bonds (calculated as ca. 3.0 Å). These features are supposed to contribute for the stabilization of the complex IV.

3.2. Complexation energies

The calculated binding energies (uncorrected for BSSE) of the complexes I–IV at different levels of DFT are given in the first entry of Table 3. Correspondingly to these

Table 1
Calculated properties of the glycine dimers I–IV using different levels of DFT

H-Bonds (Å)		I		II		III		IV	
		B1	B2	B1	B2	B1	B2	B1	B2
O–H···O=C	B3LYP	1.684[a]	1.651	–	–	–	–	–	–
	B3PW91	1.644[a]	1.616	–	–	–	–	–	–
	mPW1PW91	1.641[a]	1.614	–	–	–	–	–	–
	MP2		1.661	–	–	–	–	–	–
O–H···N<	B3LYP	–	–	1.745	1.729	1.747	1.736	1.904 [a,b]	1.892[b]
	B3PW91	–	–	1.704	1.693	1.710	1.703	1.856[a,b]	1.841 [b]
	mPW1PW91	–	–	1.699	1.689	1.705	1.698	1.855[b]	1.842[b]
	MP2	–	–	–	–	–	1.702	–	1.859[b]
N–H···O=C	B3LYP	–	–	2.419	2.441	–	–	2.293	2.289
	B3PW91	–	–	2.396	2.392	–	–	2.286	2.280[a]
	mPW1PW91	–	–	2.368	2.369	–	–	2.259	2.249
	MP2	–	–	–	–	–	–	–	2.281[b]
C–H···O=C	B3LYP	–	–	–	–	2.418	2.413	–	–
	B3PW91	–	–	–	–	2.401	2.395	–	–
	mPW1PW91	–	–	–	–	2.378	2.371	–	–
	MP2	–	–	–	–	–	2.429	–	–
C–H···O–H	B3LYP	–	–	–	–	–	–	2.956[a]	2.934[a]
	B3PW91	–	–	–	–	–	–	2.936[a]	2.922[a]
	mPW1PW91	–	–	–	–	–	–	2.889[a]	2.877[a]
	MP2	–	–	–	–	–	–	–	2.770[a]
Rotational constants (GHz)									
I_A	B3LYP	3.97807	4.03044	3.96738	3.74909	3.65581	3.62799	1.70119	1.68920
	B3PW91	4.00462	4.05656	4.08160	3.99673	3.68820	3.65939	1.70976	1.68986
	mPW1PW91	4.02263	4.06887	4.07984	3.97221	3.70251	3.67041	1.73100	1.70965
	MP2	–	3.94804	–	–	–	3.46594	–	1.76056
I_B	B3LYP	0.46412	0.46464	0.36618	0.37506	0.39657	0.39730	0.92430	0.92691
	B3PW91	0.47243	0.47167	0.36801	0.37052	0.40141	0.40203	0.93152	0.93379
	mPW1PW91	0.47431	0.47901	0.37153	0.37498	0.40478	0.40559	0.94903	0.95358
	MP2	–	0.46462	–	–	–	0.41551	–	0.99444
I_C	B3LYP	0.42036	0.42079	0.36168	0.37148	0.37356	0.37459	0.75169	0.75197
	B3PW91	0.42707	0.42668	0.36356	0.36658	0.37845	0.37931	0.75642	0.75495
	mPW1PW91	0.42879	0.42864	0.36727	0.37148	0.38177	0.38281	0.77279	0.77385
	MP2	–	0.42034	–	–	–	0.39941	–	0.81818
Dipole moments (D)									
μ	B3LYP	2.695	2.565	3.463	3.268	3.011	2.912	0.025	0.023
	B3PW91	2.723	2.587	3.684	3.550	3.154	3.044	0.021	0.003
	mPW1PW91	2.730	2.598	3.639	3.502	3.109	3.003	0.024	0.002
	MP2	–	2.671	–	–	–	2.799	–	0.001

B1 = 6-311+G(d,p), B2 = aug-cc-pVDZ.
[a] Average values between two equivalent H-bonds.
[b] Intramolecular H-bond.

Table 2
Relative stabilities (kcal/mol) for the different glycine dimers with respect to the total energy of dimer I

Dimers	B3LYP		B3PW91		mPW1PW91		MPW1B95	MP2
	6-311+G(d,p)	aug-cc-pVDZ	6-311+G(d,p)	aug-cc-pVDZ	6-311+G(d,p)	aug-cc-pVDZ	aug-cc-pVTZ	aug-cc-pVDZ
I	0.00	0.00	0.00	0.00	0.00	0.00	0.00	0.00
II	4.52	5.22	4.27	4.99	4.49	5.17	5.02	–
III	3.08	4.13	2.90	4.00	3.12	4.19	4.43	2.52
IV	3.90	4.74	3.58	4.52	3.24	4.18	1.66	–1.33

calculations, we have also presented the BSSE, NRE, and ΔZPVE corrections in the next three entries of Table 3. For all DFT methods considered, dimer I was found as the most strongly bound complex in the studied series, giving binding energy differences around 6 kcal mol^{-1} with respect to dimer IV, after correcting for BSSE and ΔZPVE. In practice, dimers II and III are not well separated in terms of their binding energies. Concerning the geometries

Table 3
Binding energy (BE), basis set superposition error (BSSE), nuclear relaxation energy (NRE), and zero-point vibrational energy (ZPVE) calculated at different levels of DFT for the glycine dimers I–IV

Dimer	BE		BSSE		NRE		ΔZPVE	
	B3LYP/B1	B3LYP/B2	B3LYP/B1	B3LYP/B2	B3LYP/B1	B3LYP/B2	B3LYP/B1	B3LYP/B2
I	−15.77	−15.91	−0.88	−0.64	3.03	3.51	1.32	1.34
II	−11.24	−10.69	−0.81	−0.58	1.46	1.45	1.37	1.31
III	−11.29	−10.87	−0.75	−0.67	1.71	1.80	1.40	1.26
IV	−9.80	−9.78	−0.41	−0.68	1.03	0.92	1.56	0.97
	B3PW91/B1	*B3PW91/B2*	*B3PW91/B1*	*B3PW91/B2*	*B3PW91/B1*	*B3PW91/B2*	*B3PW91/B1*	*B3PW91/B2*
I	−15.49	−15.54	−1.04	−0.64	3.65	4.17	1.18	1.26
II	−11.23	−10.56	−0.91	−0.57	1.75	1.73	1.32	1.29
III	−11.13	−10.58	−0.97	−0.64	2.09	2.05	1.34	1.22
IV	−8.87	−8.59	−0.57	−0.85	1.07	1.17	1.45	0.85
	mPW1PW91/B1	*mPW1PW91/B2*	*mPW1PW91/B1*	*mPW1PW91/B2*	*mPW1PW91/B1*	*mPW1PW91/B2*	*mPW1PW91/B1*	*mPW1PW91/B2*
I	−16.53	−16.53	−1.10	−0.65	3.53	4.06	1.20	1.25
II	−12.04	−11.36	−0.95	−0.59	1.71	1.69	1.33	1.30
III	−12.03	−11.44	−1.04	−0.66	2.06	2.00	1.35	1.21
IV	−10.42	−10.06	−0.89	−0.93	1.29	1.16	1.47	0.88
	MPW1B95/B3	*MP2/B2*			*MPW1B95/B3*	*MP2/B2*		
I	−15.61	−17.26			3.12	2.74		
II	−10.59				1.31			
III	−10.69	−13.84			1.47	1.80		
IV	−12.03	−17.16			1.16	0.82		

All values in kcal mol^{-1}.
B1 = 6-311+G(d,p), B2 = aug-cc-pVDZ, B3 = aug-cc-pVTZ.

of II and III, we recall that the O–H···N< hydrogen bonds in both structures seems to equally contribute to the stabilization of the complexes, having a secondary contribution of the N–H···O=C (dimer II) or C–H···O=C (dimer III) hydrogen bonds, what is corroborated by ρ_{HB} values shown in Fig. 1 (see Section 3.3). Then, a similar hydrogen bonding pattern seems to explain the same binding energy in both dimers.

We have found the binding energy of dimer IV to be higher than expected, since the stacked structure presents both longer and weaker hydrogen bonds (Table 1). Considering the usual DFT calculations, this is only 1–2 kcal/mol smaller in comparison with dimers II or III. In fact, the dipole–dipole interaction in the stacked structure plays an important role in the stabilization of IV, which seems to be dominated much more by dispersion energy than hydrogen bonding. This result is confirmed by the larger binding energy obtained with MPW1B95 calculations (−12.0 kcal mol^{-1}), which exceeds that of dimers II and III (−10.6 and −10.7 kcal mol^{-1}, respectively), while the value obtained for dimer I remain practically the same as those obtained at the other levels (−15.6 kcal mol^{-1}). This is also confirmed using MP2/aug-cc-pVDZ and by ρ_{HB} values (Fig. 1).

Analyzing the calculated NRE of the glycine monomers in the last entry of Table 3, we notice that the geometric deformation can produce different effects in the binding energies of the dimers. An average reduction of ca. 3.7 kcal/mol was calculated in dimer I, and ca. 1.1 kcal/mol in dimer IV. In this sense, including NRE in the binding energy diminished significantly the relative bond strength of dimer I compared to the other structures. The smaller difference between I and IV is now calculated as 3.2 kcal/mol at the B3LYP/aug-cc-pVDZ level, whereas the largest difference is calculated as 3.9 kcal/mol at the mPW1PW91/6-311+G(d,p) level. Even though taking into account the NRE correction, dimer I was still found as the most stable structure with all the DFT functionals, while dimer IV gave the less stable structure, except for using the B3LYP/aug-cc-pVDZ and MPW1B95/aug-cc-pVTZ levels. The binding energies were calculated (in kcal/mol) as −10.4, −7.3, −7.1, and −7.2 for the structures I, II, III, and IV, respectively, in the former and −12.5, −9.3, −9.2, and −10.9 in the latter. Nevertheless, MP2 calculations provide more strongly bound dimer IV, which after NRE corrections, becomes the most strongly bound structure (−16.3 kcal/mol), exceeding the NRE corrected binding energy of dimer I (−14.5 kcal/mol).

3.3. QTAIM analysis

$\Delta N(\Omega)$ values calculated for all the dimers, shown in Fig. 1, indicate that the formation of asymmetric dimers (II and III) is accompanied by an electron density transference from one monomer to another (0.060 au in both cases with MPW1B95 and 0.071 au in III with MP2). In spite of its small magnitude, this electron transference can be considered significant because of: (i) it is much larger than the

error attained for recovering total molecular electron populations (Section 2); and (ii) its magnitude is in line with those computed for the formation of similar dimers and adducts stabilized by H-bonds [35].

In both cases, the electron density is transferred from the monomer whose amino group is involved in hydrogen bonding, whereas the monomer that employs its carboxylic group in hydrogen bonds increases its electron density. Contrary to what is usually found [22], the monomer that receives electron density becomes destabilized in the dimer with regard to its isolated form. Thus, in dimer III, the summation of $E(\Omega)$ values of the *ASA* glycine monomer (acceptor monomer) is 12 kJ mol^{-1} less negative than in the isolated monomer, and that of the *AAA* glycine monomer (donor of electron density) is 57 kJ mol^{-1} more negative. In the same vein, dimer II, made up by two *AAG* monomers, displays an electron density donor estabilization of 62 kJ mol^{-1} that exceeds the acceptor destabilization (18 kJ mol^{-1}).

As could be expected, nearly symmetric dimers (I and IV) display neutral monomers. Each of them experiences half of the dimer stabilization with regard to the energy of the isolated glycine monomer. Looking at $\Delta N(\Omega)$ values, we observe that the largest variations of dimer I are concentrated in –COOH groups, where H and C electron populations are depleted whereas both N(O) values are enhanced. –COOH and –CH_2NH_2 groups are practically neutral in this dimer, although the former stabilizes much more (23 kJ mol^{-1}) than the latter (9 kJ mol^{-1}). If we exclude one of the CH_2 hydrogens, all the atoms of dimer IV experience significant $N(\Omega)$ variations with regard to the *SSS* isolated glycine monomer. It has to be noticed that C=O···H–N bonds involve larger $\Delta N(\Omega)$ values than >O···H–C ones.

Finally, ρ_{HB} values shown in Fig. 1 can be taken as a measure of the relative strength of H-bonds [22]. This allows us to distinguish between 4 relatively strong H-bonds ($\rho_{H\text{-}BCP}$ around 0.05 au) and 6 rather weak ones (ρ_{HB} around 0.01 au). The former are the two established between monomers in dimer I and the O–H···N H-bonds observed in dimers II and III. All of them are close to linear X–H···Y angles (179.5°, 167.9°, and 172.6° in, respectively,

Table 4
Vibrational analysis of the glycine dimers I–IV using different levels of DFT calculations

Stretching modes (cm^{-1})		I		II		III		IV	
		B1	B2	B1	B2	B1	B2	B1	B2
O–H (1)	B3LYP	3147^{s}	3043^{s}	2983^{b}	2944 ^{b}	2984^{b}	2945^{b}	3401^{s}	3368^{s}
	B3PW91	3066^{s}	2957^{s}	2907^{b}	2868^{b}	2911^{b}	2877^{b}	3353^{s}	3311^{s}
	mPW1PW91	3107^{s}	3001^{s}	2941^{b}	2902^{b}	2943^{b}	2909^{b}	3395^{s}	3358^{s}
O–H (2)	B3LYP	3240^{a}	3151^{a}	3758^{f}	3741 ^{f}	3756^{f}	3740^{f}	3404^{a}	3371^{a}
	B3PW91	3175^{a}	3082^{a}	3786^{f}	3767^{f}	3784^{f}	3766^{f}	3357^{a}	3314^{a}
	mPW1PW91	3212^{a}	3122^{a}	3819^{f}	3800^{f}	3817^{f}	3799^{f}	3399^{a}	3362^{a}
N–H (1) (sym.)	B3LYP	3519	3504	3478^{b}	3471^{b}	3488 ^{b}	3477^{b}	3498	3487
	B3PW91	3538	3521	3494^{b}	3484^{b}	3509^{b}	3497 ^{b}	3514	3503
	mPW1PW91	3562	3546	3517^{b}	3508^{b}	3533^{b}	3521^{b}	3538	3525
N–H (2) (sym.)	B3LYP	3519	3504	3512^{f}	3497^{f}	3514 ^{f}	3499^{f}	3498	3488
	B3PW91	3538	3521	3528^{f}	3510^{f}	3535^{f}	3519 ^{f}	3515	3504
	mPW1PW91	3562	3546	3553^{f}	3535^{f}	3560^{f}	3543^{f}	3539	3526
N–H (1) (antisym.)	B3LYP	3605	3595	3560^{b}	3560^{b}	3554^{b}	3546^{b}	3600	3593
	B3PW91	3631	3617	3579^{b}	3576^{b}	3578^{b}	3570 ^{b}	3624	3617
	mPW1PW91	3656	3643	3604^{b}	3602^{b}	3603^{b}	3595^{b}	3650	3642
N–H (2) (antisym.)	B3LYP	3605	3595	3603^{f}	3592^{f}	3586^{f}	3574^{f}	3600	3593
	B3PW91	3631	3617	3627^{f}	3613^{f}	3611^{f}	3597 ^{f}	3624	3617
	mPW1PW91	3656	3643	3653^{f}	3636^{f}	3636^{f}	3622^{f}	3650	3642
C=O (1)	B3LYP	1716^{s}	1703^{s}	1769^{b}	1760 ^{b}	1759^{b}	1749^{b}	1802^{s}	1794^{s}
	B3PW91	1725^{s}	1711^{s}	1785^{b}	1774^{b}	1778^{b}	1767^{b}	1822^{s}	1813^{s}
	mPW1PW91	1742^{s}	1729^{s}	1802^{b}	1792^{b}	1796^{b}	1785^{b}	1838^{s}	1829^{s}
C=O (2)	B3LYP	1763^{a}	1753^{a}	1820^{f}	1810 ^{f}	1812^{f}	1802^{f}	1825^{a}	1815^{a}
	B3PW91	1780^{a}	1769^{a}	1839^{f}	1828^{f}	1832^{f}	1821^{f}	1844^{a}	1834^{a}
	mPW1PW91	1798^{a}	1787^{a}	1857^{f}	1846^{f}	1850^{f}	1838^{f}	1862^{a}	1853^{a}
Bending modes (cm^{-1})									
NH_2 (1)	B3LYP	1639	1618	1643^{b}	1610^{b}	1670 ^{b}	1646^{b}	1657	1635
	B3PW91	1636	1614	1638^{b}	1609^{b}	1666^{b}	1644 ^{b}	1651	1631
	mPW1PW91	1645	1624	1647^{b}	1617^{b}	1675^{b}	1653^{b}	1659	1638
NH_2 (2)	B3LYP	1640	1618	1638^{f}	1614^{f}	1678 ^{f}	1655^{f}	1660	1639
	B3PW91	1636	1615	1635^{f}	1611^{f}	1675^{f}	1654 ^{f}	1655	1635
	mPW1PW91	1646	1624	1645^{f}	1621^{f}	1685^{f}	1663^{f}	1663	1643

B1 = 6-311+G(d,p), B2 = aug-cc-pVDZ. ^{s}Symmetric, ^{a}antisymmetric, ^{b}H-bonded, and ^{f}free vibrational modes. (1) and (2) refer to the different monomers of glycine in the dimers.

dimers I, II, and III). All the weak ones display much lower X–H···Y angles (from 122° to 130°). Dimers II and III show one weak H-bond each, whereas the four H-bonds observed in stacked dimer IV are of this kind.

3.4. Vibrational analysis

We have computed the harmonic vibrational frequencies for dimers I–IV, as well as for their corresponding monomers, using the common DFT levels of calculation. The most important frequencies are listed in Table 4 only for the dimer structures. The largest red shifts calculated for the O–H stretches in dimer I with respect to the isolated monomer were 722 cm^{-1} (symmetric vibration) and 613 cm^{-1} (antisymmetric vibration) using B3PW91/6-311+G(d,p). Similar results of 714 and 609 cm^{-1} were obtained using mPW1PW91/6-311+G(d,p). With B3LYP/6-311+G(d,p) it follows that these vibrational modes were less red-shifted giving 612 and 519 cm^{-1}, respectively, for both modes. In Ref. [15], the lower limits of the corresponding shifts of the symmetric and antisymmetric modes were calculated at 512 and 421 cm^{-1}, while its best estimate for the shift in the infrared active antisymmetric O–H stretch was 567 cm^{-1}. This result is in line with our calculated value of 612 cm^{-1} at the B3LYP/6-311+G(d,p) level, without using any scaling-factor of frequency.

For the stacked structure (dimer IV), the red shift in the symmetric O–H stretch, compared to its isolated monomer, was calculated as 88 cm^{-1}; and 85 cm^{-1} for the symmetric mode using B3LYP/6-311+G(d,p). A larger red shift in the O–H stretch of 270 cm^{-1} can be estimated for dimer IV, as compared to the corresponding stretch in the glycine monomer within the conformation of dimer I, having an intramolecular O–H···N hydrogen bond. Analyzing the B3LYP/6-311+G(d,p) level, large red shifts were calculated for dimers II (776 cm^{-1}) and III (767 cm^{-1}), which also give evidence of the formation of a strong hydrogen bonding patterns.

As can be noticed in our analysis, the calculated vibrational spectra of dimers I–III using different DFT levels give evidence of the formation of strong hydrogen bonds involving two O–H···O=C. On the other hand, these calculations revealed only small changes in the vibrational modes of dimer IV. For instance, using mPW1PW91/aug-cc-pVDZ, the antisymmetric N–H stretching frequencies involved in the supposed hydrogen bonds of this structure was red-shifted by only 2 cm^{-1} with respect to the same mode in the isolated monomer. Similarly, the antisymmetric C–H stretches (calculated at 3136 cm^{-1}) were red-shifted by 3 cm^{-1}. The largest shifts were calculated using the 6-311+G(d,p) basis set with all these functionals. In the case of B3LYP, we obtained red shifts of 15 and 39 cm^{-1} for the antisymmetric and symmetric N–H stretches, respectively. Correspondingly, red shifts of 7 cm^{-1} were calculated for both the antisymmetric and symmetric C–H stretching frequencies.

4. Summary and conclusions

This Letter has investigated the stability and hydrogen bonding of structurally different glycine dimers using different levels of calculations. Considering the usual DFT methods, dimer I (containing two linear O–H···O intermolecular hydrogen bonds) was found to be the most strongly bound structure in the studied series I–IV. Its binding energy differences with respect to dimer IV were calculated in the range of 5.7–6.4 kcal/mol, after BSSE and ΔZPVE corrections. On the other hand, this difference is reduced to 3.6 kcal/mol with MPW1B95/aug-cc-pVTZ and to 0.1 kcal/mol with MP2/aug-cc-pVDZ.

Dimer IV was surprisingly calculated as a rather stable structure, with binding energy similar to those for structures II and III. This is evidenced in the QTAIM calculations for the complexation of the stacked structure. Also, this is confirmed using the MP2/aug-cc-pCVD method. Improving the computational level for a better description of dispersion effects (MPW1B95 and MP2 calculations) increases the stability of dimer IV with regard to dimer I. In fact dimer IV was found to be 1.33 kcal/mol more stable than dimer I at the MP2/aug-cc-pVDZ level.

Finally, as obtained from the harmonic approximation calculation, the O–H stretching modes of the structures I–III yielded large red shifts, which are compatible with the strength the hydrogen bonds formed in these structures. However, taking into account the small differences in binding energy, the calculated frequency shifts cannot be decisive to point out the most stable structure.

Acknowledgements

We thank CENAPAD-SP for the use of computational facilities. This work has been partially supported by FAPESB and CNPq.

References

[1] J.U. Bowie, Nature 438 (2005) 581.
[2] A. Grottesi, C. Domene, B. Hall, M.S.P. Sansom, Biochemistry 44 (2005) 14594.
[3] R. Wieczorek, J.J. Dannenberg, J. Am. Chem. Soc. 125 (2003) 8124.
[4] R. Wieczorek, J.J. Dannenberg, J. Am. Chem. Soc. 125 (2003) 14065.
[5] K. Akasaka, Pure Appl. Chem. 75 (2003) 927.
[6] C.D. Keefe, J.K. Pearson, J. Mol. Struct. (Theochem) 679 (2004) 65.
[7] P. Chaudhuri, S. Canuto, J. Mol. Struct. (Theochem) 760 (2006) 15.
[8] R. Ramaekers, J. Pajak, B. Lambie, G. Maesa, J. Chem. Phys. 120 (2004) 4182.
[9] B.M. Messer, C.D. Cappa, J.D. Smith, K.R. Wilson, M.K. Gilles, R.C. Cohen, R.J. Saykally, J. Phys. Chem. B 109 (2005) 5375.
[10] C.M. Aikens, M.S. Gordon, J. Am. Chem. Soc. 128 (2006) 12835.
[11] P.D. Godfrey, R.D. Brown, J. Am. Chem. Soc. 117 (1995) 2019.
[12] S.J. McGlone, P.S. Elmes, R.D. Brown, P.D. Godfrey, J. Mol. Struct. 485-486 (1999) 225.
[13] A.G. Császár, J. Am. Chem. Soc. 114 (1992) 9568.
[14] J.J. Neville, Y. Zheng, C.E. Brion, J. Am. Chem. Soc. 118 (1996) 10533.
[15] J. Chocholoušsová, J. Vacek, F. Huisken, O. Werhahn, P. Hobza, J. Phys. Chem. A 106 (2002) 11540.

[16] S. Scheiner, Hydrogen Bonding: A Theoretical Perspective, Oxford University Press, New York, 1997.
[17] R. Rivelino, S. Canuto, J. Phys. Chem. A 105 (2001) 11260.
[18] K. Koch, M.C. Holthausen, A Chemists Guide to Density Functional Theory, Wiley, VCH, Weinheim, 2001.
[19] R. Miao, C. Jin, G. Yang, J. Hong, C. Zhao, L. Zhu, J. Phys. Chem. A 109 (2005) 2340.
[20] R. Rivelino, V. Ludwig, E. Rissi, S. Canuto, J. Mol. Struct. 615 (2002) 257.
[21] R. Rivelino, S. Canuto, J. Phys. Chem. A 108 (2004) 1601.
[22] R.F.W. Bader, Atoms in Molecules, a Quantum Theory, Oxford University Press, New York, 1990.
[23] M.J. Frisch et al., GAUSSIAN 98, Revisions A.7 and A.11.4, Gaussian, Inc., Pittsburgh, PA, 1998.
[24] M.J. Frisch et al., GAUSSIAN 03, Revision C.02, Gaussian, Inc., Wallingford CT, 2004.
[25] A.D. Becke, J. Chem. Phys. 98 (1993) 5648.
[26] C. Lee, W. Yang, R.G. Parr, Phys. Rev. B 37 (1988) 785.
[27] J.P. Perdew, Y. Wang, Phys. Rev. B 45 (1992) 13244.
[28] A.D. Becke, Phys. Rev. A 38 (1988) 3098.
[29] C. Adamo, V. Barone, J. Chem. Phys. 108 (1998) 664.
[30] Y. Zhao, D.G. Truhlar, J. Phys. Chem. A 108 (2004) 6908.
[31] M.J. González Moa, M. Mandado, R.A. Mosquera, J. Phys. Chem. A 111 (2007) 1998.
[32] S.F. Boys, F. Bernardi, Mol. Phys. 19 (1970) 553.
[33] F.B. van Duijneveldt, J.G.C.M. van Duijneveldt-van de Rijdt, J.H. van Lente, Chem. Rev. 94 (1994) 1873.
[34] R.F.W. Bader, AIMPAC: A suite of programs for the theory of atoms in molecules, McMaster University, Hamilton, Ontario, Canada, 1994.
[35] A. Vila, R.A. Mosquera, Chem. Phys. 291 (2003) 73.